Synergistic effect of two inhibitors on one activator in a reaction-diffusion system

Satoshi Kawaguchi[1] and Masayasu Mimura[2]
[1]*Department of Complex Systems, School of Systems Information Science, Future University-Hakodate, Hakodate 041-8655, Japan*
[2]*Department of Mathematics, School of Science and Technology, Meiji University, Kawasaki 214-8571, Japan*
(Received 8 December 2007; revised manuscript received 4 February 2008; published 3 April 2008)

We investigate a three-component reaction-diffusion system that describes the interaction of one activator and two inhibitors where one inhibitor acts as a traveling pulse generator of the activator and the other acts as a lateral inhibition localizer. It is numerically shown that the synergistic effect of these two inhibitors on one activator induces several spatiotemporal patterns such as destabilization and nonannihilation of traveling pulses and the occurrence and splitting of traveling spots. By using singular perturbation procedures, the stability of radially symmetric equilibrium solutions is discussed. Furthermore, we discuss how such dynamics are caused under the synergistic effect of two inhibitors.

DOI: 10.1103/PhysRevE.77.046201 PACS number(s): 89.75.Kd, 05.45.−a, 05.70.Ln

I. INTRODUCTION

Reaction-diffusion (RD) systems have been proposed to describe a wide range of spatiotemporal patterns arising in physics [1–3], chemistry [4–6], biology [7–9], and other applied sciences. Among such RD systems, there are some that describe the interaction of activators and inhibitors to study pattern formation arising in far-from-equilibrium states [10,11]. In particular, several two-component systems with one-activator and one-inhibitor systems have been theoretically investigated by many authors ([12–18], for instance).

A well-studied system for one activator u and one inhibitor v is

$$\epsilon\sigma u_t = \epsilon^2\nabla^2 u + f(u,v), \tag{1.1}$$

$$t>0, \quad \mathbf{x}\in R^n \quad (n=1,2),$$

$$v_t = \nabla^2 v + g(u,v), \tag{1.2}$$

where $f(u,v)=u(1-u)(u-a)-v$ with $0<a<1/2$ and $g(u,v)=\mu u-v$ with $\mu>0$, $\sigma>0$, and $\epsilon>0$. Here, ϵ is an important parameter that is sufficiently small. Suppose that $f(u,v)=0$ and $g(u,v)=0$ have one intersection point in the $(u,\ v)$-plane, as shown in Fig. 1(a). Then, the kinetics of f and g possesses a monostable excitability mechanism. When σ is large—that is, when the diffusion rate of u is smaller than that of v—the localization of the activator occurs due to long-range inhibition, by which localized equilibrium solutions appear (we call them standing pulses in one dimension and standing spots in two dimensions). As σ decreases, the standing pulse (or spot) is destabilized through Hopf bifurcation and the resulting pulse exhibits a breathing motion, as shown in Fig. 2. When σ is small, there no longer exist stable standing pulses; instead, there appear stable traveling pulses in one dimension. The feature of these traveling pulses is that they annihilate each other when they collide, as shown in Fig. 3. In two dimensions, there is no stable traveling spot; instead, there appears an expanding wave that evolves into either an expanding ring or a pair of spirals, as shown in Fig. 4. When the radius of a standing spot becomes large, it is primarily destabilized through static bifurcation with $n=2$ mode and the standing spot splits into two standing spots, as shown in Fig. 5.

Let us introduce another one-activator and one-inhibitor system

$$\epsilon\sigma u_t = \epsilon^2\nabla^2 u + h(u,w), \tag{1.3}$$

$$t>0, \quad \mathbf{x}\in R^n,$$

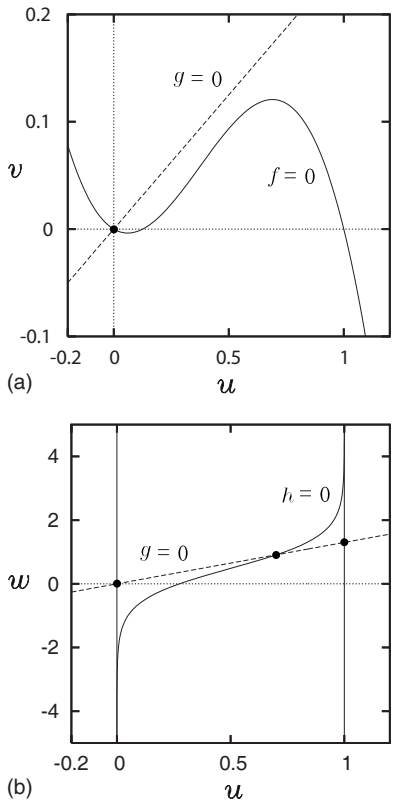

FIG. 1. One-activator and one-inhibitor RD systems. (a) Nullclines of $f=0$ and $g=0$ in Eqs. (1.1) and (1.2) ($\mu=0.25$ and $a=0.1258$). (b) Nullclines of $h=0$ and $g=0$ in Eqs. (1.3) and (1.4) ($\mu=1.3$, $\alpha=1.0$, $s_0=0.0$, and $\hat{a}_0=-0.4847$).

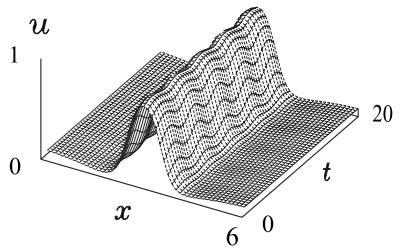

FIG. 2. A standing pulse with breathing motion in Eqs. (1.1) and (1.2) (ϵ=0.125, μ=0.25, a=0.1258, and σ=0.3308).

$$\tau w_t = d\nabla^2 w + g(u,w), \tag{1.4}$$

where $h(u,w)=u(1-u)[u-a(w)]$ with $a(w)=1/2\{1+\tanh[\alpha(w-s_0)+\hat{a}_0]\}$, and $\alpha>0$, $s_0\geq 0$, and $\hat{a}_0$ are constants. We note that the nullclines $h(u,w)=0$ and $g(u,w)=0$ have three intersection points, as shown in Fig. 1(b). Let σ be a fixed small value. If d is small, there exist stable traveling pulses that possess an annihilation property on collision, as shown in Fig. 6(a). On the other hand, if d is large, there exists no traveling pulse solution but a stable localized equilibrium solution [Fig. 6(b)]. It is obvious that Eq. (1.1) with $v=0$ and Eq. (1.3) with $w=0$ reduce to the following scalar bistable RD system for u:

$$\epsilon\sigma u_t = \epsilon^2\nabla^2 u + u(1-u)(u-a); \tag{1.5}$$

this has been investigated in detail previously (Ref. [19], for instance). One thus finds that the two systems (1.1) and (1.2) and (1.3) and (1.4) are qualitatively similar.

To the best of our knowledge, there have only been several theoretical works on multicomponent RD systems. As a three-component system with two activators and one inhibitor, Ikeda and Mimura [20] proposed a population model system for two competing prey species and one predator species, where a prey and its predator species correspond to an activator and inhibitor, respectively. By using the interfacial dynamics procedure, it is shown that the system exhibits several types of spatial and/or temporal patterns, although a two-competing species system never exhibits spatiotemporal patterns in the absence of a predator. On the other hand, several groups have recently discussed one-activator and two-inhibitors systems [21–26]. Purwins and co-workers [23,25,26] have introduced a second inhibitor into the usual one-activator and one-inhibitor RD system (1.1) and (1.2), and they have numerically shown that new pulse and spot dynamics occur in the three-component system. However,

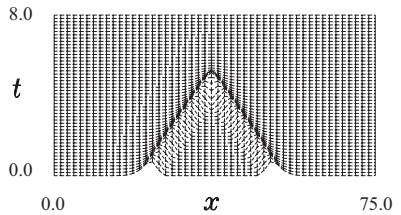

FIG. 3. Annihilation of two traveling pulses in Eqs. (1.1) and (1.2) (ϵ=0.125, μ=0.25, a=0.1258, and σ=0.12).

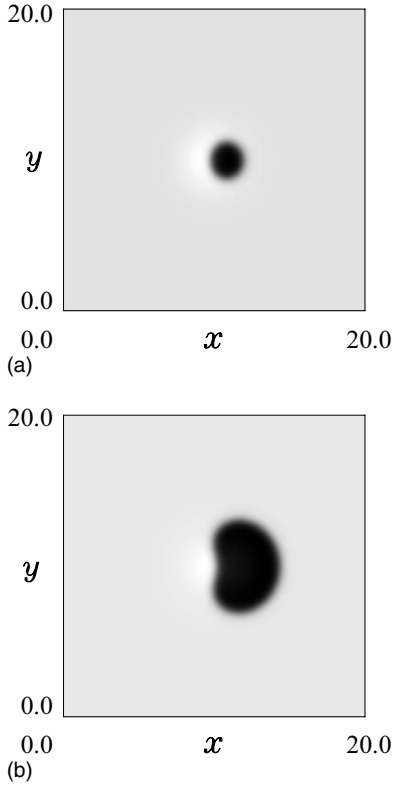

FIG. 4. An expanding wave in u component in Eqs. (1.1) and (1.2) (ϵ=0.125, μ=0.25, a=0.1258, and σ=0.05). (a) t=0.1. (b) t=0.4.

they have not theoretically explained the roles of the second inhibitor and the mechanism of these phenomena.

In this paper, we describe analytical and complementary numerical studies of the synergistic effect of two inhibitors on the occurrence of new pulse and spot behaviors. For this purpose, we propose the following three-component RD system with one activator u and two inhibitors v and w:

$$\epsilon\sigma u_t = \epsilon^2\nabla^2 u + H[u-a(w)] - u - v, \tag{1.6}$$

$$v_t = \nabla^2 v + \mu u - v, \quad t>0, \quad \mathbf{x}\in R^n, \tag{1.7}$$

$$\tau w_t = d\nabla^2 w + u + v - w - s_0, \tag{1.8}$$

with

$$a(w) = \frac{1}{2}[1+\tanh(\alpha w + \hat{a}_0)], \tag{1.9}$$

where ϵ, σ, α, τ, μ, s_0, and d are all positive constants and $H(z)$ is the step function satisfying $H(z)=0$ for $z<0$ and $H(z)=1$ for $z>0$. We note that the piecewise linear function $H(u-a)-u$ is qualitatively similar to the cubic one $u(1-u)(u-a)$ for any constant a satisfying $0<a<1$. In our computations of Eqs. (1.6)–(1.9), we assume μ=3.0, $\hat{a}_0$ =−0.4847 such that $1/2[1+\tanh(\hat{a}_0)]=a_0=0.275$, and we consider σ, τ, d, and s_0 as free parameters.

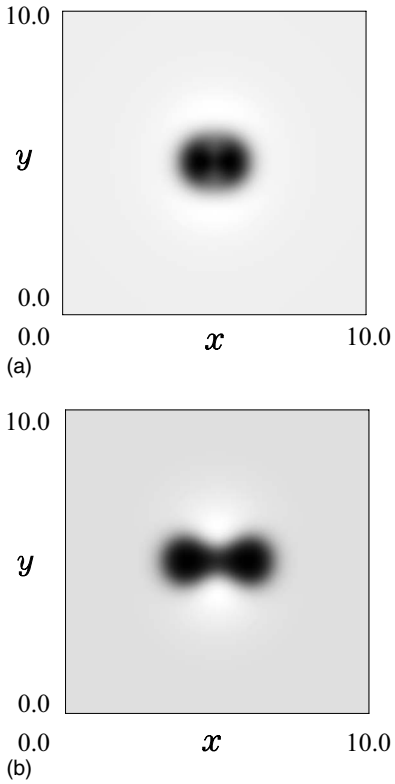

FIG. 5. Static destabilization with $n=2$ mode of a standing spot in Eqs. (1.1) and (1.2) ($\epsilon=0.125$, $\mu=0.25$, $a=0.1258$, and $\sigma=0.02$). (a) $t=0.01$. (b) $t=0.1$.

We note the following observations with regard to the above system. In the absence of w, the first two equations (1.6) and (1.7) reduce to a system similar to (1.1) and (1.2), while in the absence of v, the first and third equations (1.6) and (1.8) reduce to (1.3) and (1.4). In order to consider the synergistic effect of two inhibitors, we assume a situation where d is large and τ and σ are small. This indicates that the first inhibitor v acts as a *traveling pulse generator* and the second one w acts as a *lateral inhibition localizer* for the activator u. Second, a three-component RD system with one activator and two inhibitors is proposed as an extension of a phenomenological model of the planar dc gas-discharge system with semiconductor electrode [22,26,27]. In these systems, a cubic nonlinear term is applied for the activator. For mathematical tractability, the cubic nonlinearity is replaced by a piecewise linear function in Eq. (1.6).

We first briefly mention the dynamics of solutions to the ordinary differential equations (ODEs) corresponding to the system (1.6)–(1.9). It is obvious that there exists an equilibrium solution $(u_0,v_0,w_0)=(0,0,-s_0)$ for any s_0. In addition, if $s_0>s_0^*=(2\alpha+2\hat{a}_0+\ln\mu)/2\alpha$, there exists another solution $(u_1,v_1,w_1)=(1/\mu+1,\mu/\mu+1,1-s_0)$. Both these solutions are locally stable. In this research, we restrict s_0 to satisfy $s_0<s_0^*$. When σ and τ are both small, we find that the ODEs of (1.6)–(1.9) are a monostable system with an excitable property, as shown in Fig. 7.

We present some numerical evidences of pulse and spot dynamics arising in the system (1.6)–(1.9).

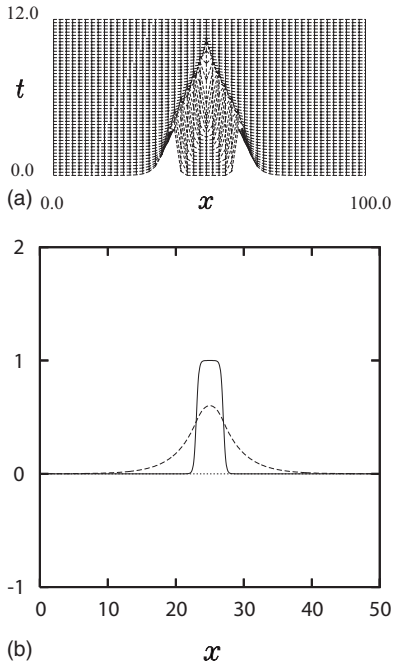

FIG. 6. Annihilation of two traveling pulses and a standing pulse in Eqs. (1.3) and (1.4). The solid and dashed curves, respectively, represent u and w ($\epsilon=0.125$, $\mu=1.3$, $\alpha=1.0$, $s_0=0.0$, $\hat{a}_0=-0.4847$, and $\sigma=0.1$). (a) Annihilation of traveling pulses ($d=1.0$ and $\tau=1.0$). (b) A standing pulse ($d=10.0$ and $\tau=0.01$).

A. Nonannihilation of traveling pulses

For s_0, α, τ, d, and σ in a suitable parameter regime, there exist stable traveling pulse solutions of Eqs. (1.6)–(1.9). The relations among the speed, pulse width, and σ are analyti-

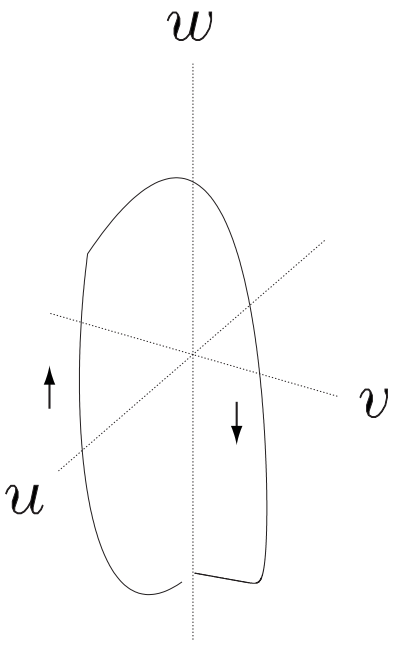

FIG. 7. Excitability of solutions to ODEs corresponding to Eqs. (1.6)–(1.9) ($\epsilon=0.125$, $\tau=0.01$, $\sigma=0.05$, $\alpha=5.0$, and $s_0=0.3$). Trajectory from the initial conditions $(u(0),v(0),w(0))=(0.05,0,-s_0)$.

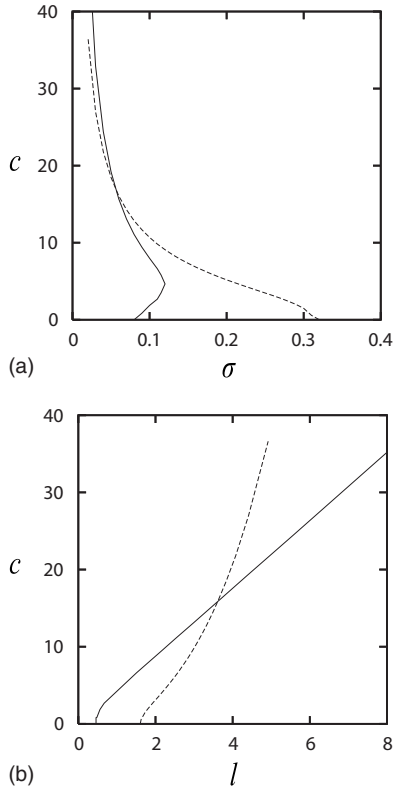

FIG. 8. Dependences of speed on σ and pulse width of traveling pulses of Eqs. (1.6)–(1.9) in the limit $\epsilon \downarrow 0$. The solid and dashed curves, respectively, represent the cases of $\alpha=0.0$ and $\alpha=3.0$ ($d=10.0$, $\tau=0.01$, and $s_0=0.34$). (a) Dependence on σ. (b) Dependence on pulse width.

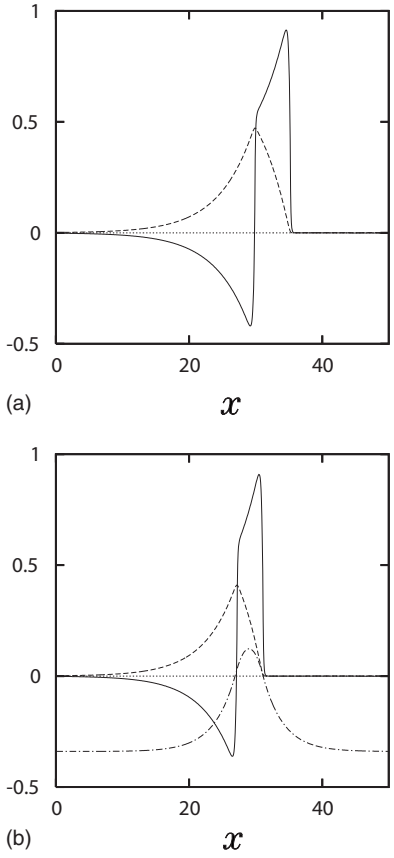

FIG. 9. Traveling pulses of Eqs. (1.6)–(1.9). The solid, dashed, and dash-dotted curves, respectively, represent u, v, and w ($\epsilon=0.125$, $d=10.0$, $\tau=0.01$, $\sigma=0.04$, and $s_0=0.34$). (a) $\alpha=0.0$. (b) $\alpha=3.0$.

cally determined in the limit $\epsilon \downarrow 0$, as shown in Fig. 8. When we choose a suitably small value of σ, we find that the speed and profiles of u and v for the case $\alpha>0$ are almost similar to those for $\alpha=0$ [that is, the two-component system (1.6) and (1.7) with $a=a_0$], as shown in Figs. 9(a) and 9(b). It appears that there is no contribution of w to the occurrence of traveling pulses. The existence and stability of traveling pulse solutions are discussed in Sec. IV.

Consider the situation where two traveling pulses approach each other. If σ is very small, they propagate so fast that they merge and disappear [Fig. 10(a)]. However, if σ increases slightly, they collide elastically [Fig. 10(b)]. Here, we should note that under the same values of parameters except for $\alpha=0$, the annihilation of traveling pulses occurs on collision [Fig. 10(c)]. This clearly indicates that the second inhibitor w plays a role in the nonannihilation property. If σ still increases, they propagate slowly and gradually stop under a repulsive force [Fig. 10(d)]. Unlike the one-activator and one-inhibitor RD system, the second inhibitor w induces a long-range interaction between the two pulses so that they form a stable bound state by numerical simulations.

Integrating the above, we conclude that the second inhibitor w does not exert so much influence on a single traveling pulse if it is far away from the others. However, when two traveling pulses approach closely, since the characteristic time τ is very small and the diffusion rate d is very large, the concentration of w in the interval between the two pulses increases so rapidly that there a braking effect occurs on traveling pulses, even if it is too far to increase the concentration of v. If the speed is so fast that it overcomes the braking effect, pair annihilation of the two traveling pulses occurs. We note that the nonannihilation of traveling pulses has already been reported in some two-component RD systems such as the Gray-Scott model [11,28,29] and FitzHugh-Nagumo system [30]. The key point for this type of nonannihilation property is that the speed is very slow [31,32]. On the other hand, for our three-component RD system, when very slowly traveling pulses approach each other, they gradually stop. If the speed is slightly faster, they reflect each other. From the above, we deduce that it is necessary for the nonannihilation property that the speed is sufficiently fast in order to overcome the repulsive force caused by the second inhibitor.

B. Traveling spots

As stated previously, when α is small, no traveling spot exists, as shown in Fig. 4. However, if α is suitably large, there exists a stable moving spot, as shown in Fig. 11(a), which propagates with constant shape and speed. We call this a traveling spot. The appearance of traveling spots in our system is intuitively explained as follows: Suppose that there

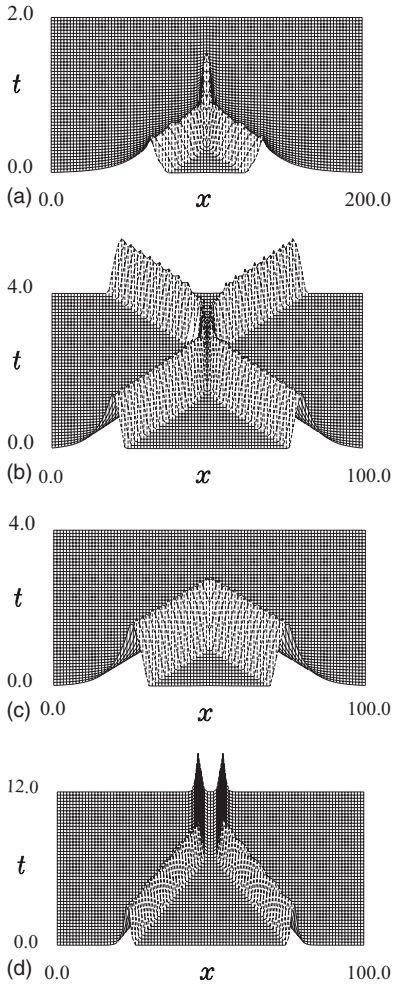

FIG. 10. Interaction of two traveling pulses (ϵ=0.125, d=10.0, τ=0.01, s_0=0.34, and α=3.0). (a) Pair annihilation (σ=0.01). (b) Elastic collision (σ=0.04). (c) Pair annihilation (α=0 and σ=0.04). (d) Two standing pulses in a bound state (σ=0.26).

is an expanding spot that moves to one direction. As τ is small and d is large, w is rapidly generated within a spot and it diffuses to cover over the interface. This long-range inhibition effect suppresses the expansion of spots, leading to the occurrence of a traveling spot. If α is too large, the inhibition effect warps the interface so that a single traveling spot splits into many spots, as shown in Fig. 11(b). One could thus expect that the occurrence of traveling spots and splitting into many spots are due to the synergistic effect of two different inhibitors on one activator.

C. Transversal destabilization of traveling pulses

In Sec. I A, we demonstrated the existence of stable traveling pulses. Here, we consider the transversal stability of traveling pulses in the channel domain $\Omega_L=\{\mathbf{x}=(x,y)\in R^2 | x\in R,\ 0<y<L\}$ with width L, where the boundary conditions at $y=0,L$ are imposed as

$$\frac{\partial u}{\partial y}=\frac{\partial v}{\partial y}=\frac{\partial w}{\partial y}=0, \quad t>0, \quad x\in R. \tag{1.10}$$

When α is small, there exist traveling pulses for small σ. It is shown that these are transversally stable, as shown in Fig. 12(a). On the other hand, when α is suitably large, there continues to exist a traveling pulse. However, this is transversally unstable due to the lateral inhibition of w, as shown in Fig. 12(b).

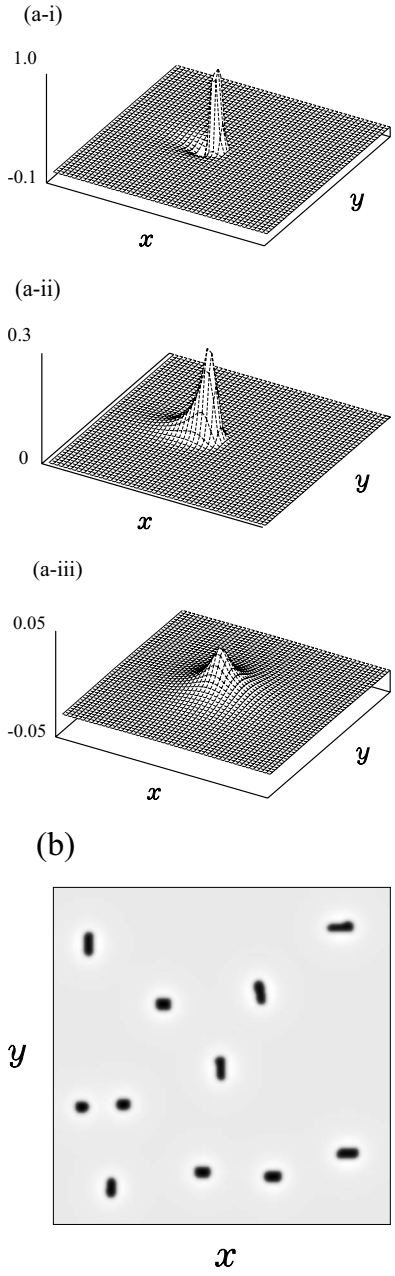

FIG. 11. A traveling spot and multispots. The domain size is 20×20 (ϵ=0.125, d=10.0, τ=0.01, s_0=0.03, and σ=0.04). (a) A traveling spot α=10.0. (a-i) u. (a-ii) v. (a-iii) w. (b) Splitting of a single traveling spot into many spots (α=60.0).

In the following sections, we discuss how these pulse and spot dynamics arising in Eqs. (1.6)–(1.9) occur under the synergistic effect of two different types of inhibitors on one activator.

II. EQUATIONS OF MOTION OF THE INTERFACE

As ϵ tends to zero, internal layers arising in the u component of Eqs. (1.6)–(1.9) become interfaces. In order to treat

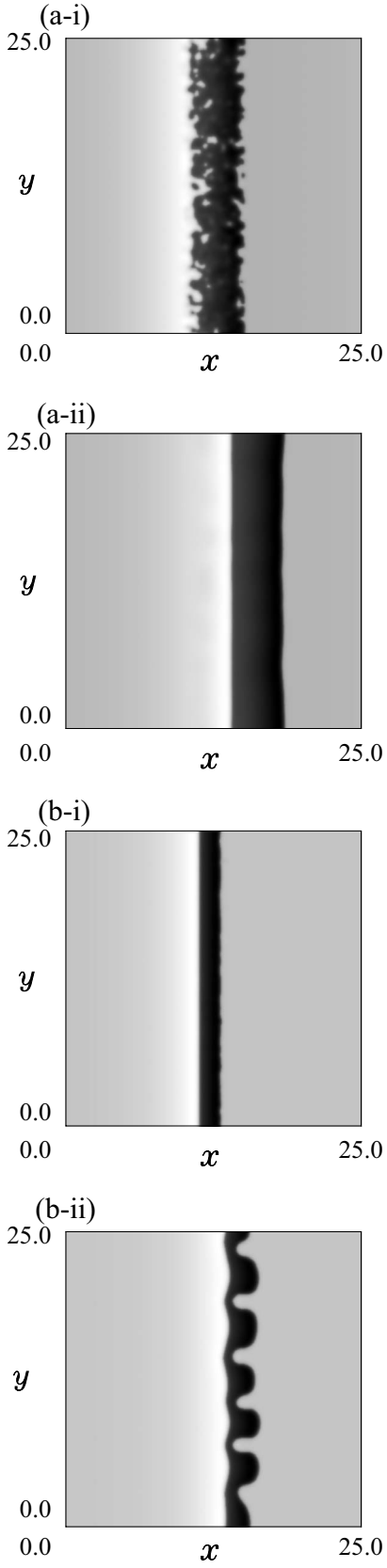

FIG. 12. Transversal stability of traveling pulses (ϵ=0.125, d=10.0, τ=0.01, s_0=0.2, σ=0.04, and L=25). (a) α=0.0. (a-i) t=0.0. (a-ii) t=0.2. (b) α=10.0. (b-i) t=0.0. (b-ii) t=0.2.

the dynamics of the patterns in Eqs. (1.6)–(1.9), we derive an evolutional equation of interfaces that is controlled by two inhibitors v and w.

Suppose that an interfacial curve—say, $\Gamma(t)$—is simply a single closed curve given in the entire plane R^2, in such a way that $R^2=\Omega_1(t)\cup\Gamma(t)\cup\Omega_0(t)$, where $\Omega_1(t)=\{(\mathbf{x},t)\in R^2\times R_+^0 | u(\mathbf{x},t)-a(w(\mathbf{x},t))>0\}$ and $\Omega_0(t)=\{(\mathbf{x},t)\in R^2\times R_+^0 | u(\mathbf{x},t)-a(w(\mathbf{x},t))<0\}$. Then, the time evolution of $\Gamma(t)$ is described by

$$\sigma\left(\frac{d\Gamma(t)}{dt}\cdot\nu\right)=C(v_i;a(w_i))-\epsilon\kappa,\quad(\mathbf{x},t)\in\Gamma(t),\quad(2.1)$$

where κ is the curvature on $\Gamma(t)$, ν is the outward normal vector on the interface $\Gamma(t)$, and v_i and w_i are the values of v and w on $\Gamma(t)$, respectively. When v and w are assumed to be constant, $C(v;a(w))$ is the velocity of the traveling front solution of the following scalar bistable RD equation for u:

$$u_t=u_{xx}+H[u-a(w)]-u-v,\quad t>0,\quad x\in R\quad(2.2)$$

with the boundary conditions

$$u(-\infty,t)=1-v\quad\text{and}\quad u(+\infty,t)=-v.\quad(2.3)$$

The velocity $C(v;a(w))$ is explicitly represented as

$$C(v;a(w))=\frac{2\left[\frac{1}{2}-v-a(w)\right]}{\{[v+a(w)][1-v-a(w)]\}^{1/2}}.\quad(2.4)$$

For the derivation of Eq. (2.1), the reader should refer to Ref. [12]. By using Eqs. (1.7) and (1.8), the equations of v and w in the limit of $\epsilon\downarrow 0$ are, respectively, given as

$$v_t=\nabla^2 v-(\mu+1)v+\mu,\quad t>0,\quad\mathbf{x}\in\Omega_1(t),$$

$$v_t=\nabla^2 v-(\mu+1)v,\quad t>0,\quad\mathbf{x}\in\Omega_0(t),\quad(2.5)$$

with the boundary conditions

$$v(\Gamma(t)-0,t)=v(\Gamma(t)+0,t),$$

$$\frac{d}{d\nu}v(\Gamma(t)-0,t)=\frac{d}{d\nu}v(\Gamma(t)+0,t),\quad t>0,$$

$$\lim_{|\mathbf{x}|\to\infty}v(\mathbf{x},t)=0,\quad(2.6)$$

and

$$\tau w_t=d\nabla^2 w+1-w-s_0,\quad t>0,\quad\mathbf{x}\in\Omega_1(t),$$

$$\tau w_t=d\nabla^2 w-w-s_0,\quad t>0,\quad\mathbf{x}\in\Omega_0(t),\quad(2.7)$$

with the boundary conditions

$$w(\Gamma(t)-0,t)=w(\Gamma(t)+0,t),$$

$$\frac{d}{d\nu}w(\Gamma(t)-0,t)=\frac{d}{d\nu}w(\Gamma(t)+0,t),\quad t>0,$$

$$\lim_{|\mathbf{x}|\to\infty} w(\mathbf{x},t) = -s_0. \tag{2.8}$$

Thus, we obtain the interface problem (2.1)–(2.8) for $(\Gamma(t), v(\mathbf{x},t), w(\mathbf{x},t))$, taking the limit $\epsilon \downarrow 0$ in Eqs. (1.6)–(1.8).

III. RADIALLY SYMMETRIC EQUILIBRIUM SOLUTIONS

We numerically find that traveling pulse solutions in one dimension and traveling spot solutions in two dimensions are bifurcated from the radially symmetric equilibrium ones. When d is large, we first show the existence of radially symmetric equilibrium solutions $(\eta_0,\ \bar{v}(r),\ \bar{w}(r))$ with $r=|\mathbf{x}|$ of Eqs. (2.1)–(2.8), where $r=\eta_0$ is the equilibrium interface position (Fig. 13), depending on the parameters s_0 and α.

Consider the stationary problem of Eqs. (2.1)–(2.8). Equation (2.1) with Eq. (2.4) immediately leads to

$$\frac{1}{2} - \bar{v}_i - a(\bar{w}_i) = 0, \tag{3.1}$$

where $\bar{v}_i=\bar{v}(\eta_0)$ and $\bar{w}_i=\bar{w}(\eta_0)$ so that Eq. (1.9) is

$$a_i = \frac{1}{2}[1 + \tanh(\alpha \bar{w}_i + \hat{a}_0)] \tag{3.2}$$

and the relation among α, η_0, $\bar{v}_i$, and $\bar{w}_i$ is given by

$$\alpha = \frac{-\hat{a}_0 - \frac{1}{2}\ln\left(\frac{2\bar{v}_i + 1}{-2\bar{v}_i + 1}\right)}{\bar{w}_i}. \tag{3.3}$$

The stationary problems corresponding to Eqs. (2.5)–(2.8) are given as

$$0 = v_{rr} + \frac{n-1}{r} v_r - (\mu+1)v + \mu, \quad 0 < r < \eta_0,$$

$$0 = v_{rr} + \frac{n-1}{r} v_r - (\mu+1)v, \quad \eta_0 < r < \infty, \tag{3.4}$$

with the boundary conditions

$$\frac{dv}{dr}(0) = 0,$$

$$v(\eta_0) = \bar{v}_i,$$

$$\frac{dv}{dr}(\eta_0 - 0) = \frac{dv}{dr}(\eta_0 + 0),$$

$$\lim_{r\to\infty} v(r) = 0, \tag{3.5}$$

and

$$0 = dw_{rr} + \frac{n-1}{r} w_r + 1 - w - s_0, \quad 0 < r < \eta_0,$$

$$0 = dw_{rr} + \frac{n-1}{r} w_r - w - s_0, \quad \eta_0 < r < \infty, \tag{3.6}$$

with

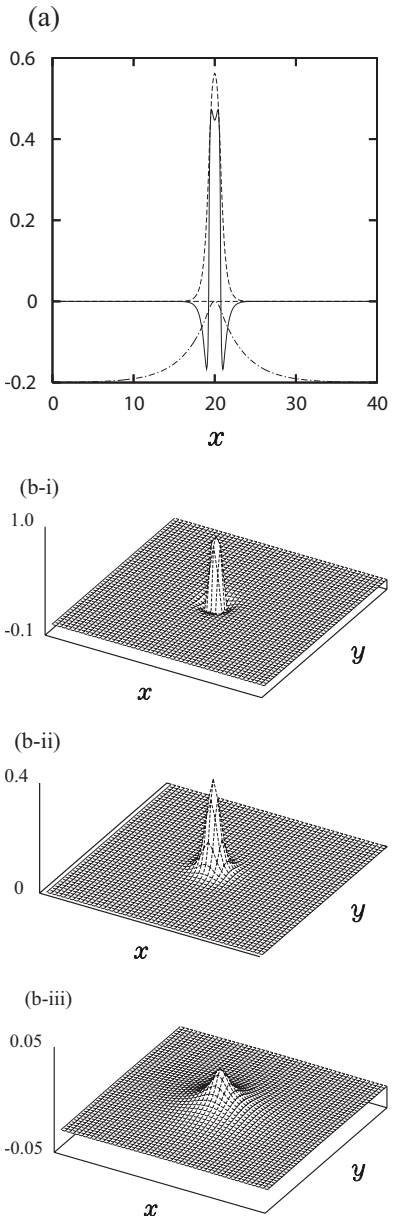

FIG. 13. Standing pulse and standing spot. (a) A standing pulse. The solid, dashed, and dash-dotted curves, respectively, represent u, v, and w (ϵ=0.125, d=10.0, τ=0.01, s_0=0.2, α=10.0, and σ=0.8). (b) A standing spot. The domain size is 20×20 (ϵ=0.125, d=10.0, τ=0.01, s_0=0.03, α=10.0, and σ=0.8). (b-i) u. (b-ii) v. (b-iii) w.

$$\frac{dw}{dr}(0) = 0,$$

$$w(\eta_0) = \bar{w}_i,$$

$$\frac{dw}{dr}(\eta_0 - 0) = \frac{dw}{dr}(\eta_0 + 0),$$

$$\lim_{r\to\infty} w(r) = -s_0. \tag{3.7}$$

Then, for fixed η_0, $(\bar{v}(r),\ \bar{w}(r))$ of Eqs. (3.4)–(3.7) are given as follows.

(i) One dimension ($n=1$):

$$\bar{v}(r)=\begin{cases}\left(\frac{\mu}{\mu+1}\right)-\left(\frac{\mu}{\mu+1}\right)e^{-\sqrt{1+\mu}\eta_0}\cosh(\sqrt{1+\mu}r), & 0<r<\eta_0,\\ \left(\frac{\mu}{\mu+1}\right)\sinh(\sqrt{1+\mu}\eta_0)e^{-\sqrt{1+\mu}r}, & \eta_0<r<\infty,\end{cases} \tag{3.8}$$

and

$$\bar{w}(r)=\begin{cases}1-s_0-e^{-\eta_0/\sqrt{d}}\cosh\left(\frac{r}{\sqrt{d}}\right), & 0<r<\eta_0,\\ -s_0+\sinh\left(\frac{\eta_0}{\sqrt{d}}\right)e^{-r/\sqrt{d}}, & \eta_0<r<\infty.\end{cases} \tag{3.9}$$

(ii) Two dimensions ($n=2$):

$$\bar{v}(r)=\begin{cases}\left(\frac{\mu}{\mu+1}\right)-\frac{\mu\eta_0}{\sqrt{\mu+1}}K_1(\sqrt{\mu+1}\eta_0)I_0(\sqrt{\mu+1}r), & 0<r<\eta_0,\\ \frac{\mu\eta_0}{\sqrt{\mu+1}}I_1(\sqrt{\mu+1}\eta_0)K_0(\sqrt{\mu+1}r), & \eta_0<r<\infty,\end{cases} \tag{3.10}$$

and

$$\bar{w}(r)=\begin{cases}-K_1(\eta_0/\sqrt{d})(\eta_0/\sqrt{d})I_0(r/\sqrt{d})+(1-s_0), & 0<r<\eta_0,\\ I_1(\eta_0/\sqrt{d})(\eta_0/\sqrt{d})K_0(r/\sqrt{d})-s_0, & \eta_0<r<\infty,\end{cases} \tag{3.11}$$

where I_n and K_n are the modified Bessel functions.

By substituting $\bar{v}_i=\bar{v}(\eta_0)$ of Eq. (3.4) and $\bar{w}_i=\bar{w}(\eta_0)$ of Eq. (3.6) into Eq. (3.3), the value of η_0 is determined. We thus obtain the solution $(\eta_0,\ \bar{v}(r),\ \bar{w}(r))$ of Eqs. (2.1)–(2.8). For the one-dimensional problem, the relation between α and η_0 for suitably fixed s_0 and d is shown in Fig. 14. The situation is classified into two cases depending on the values of s_0. For small s_0 (<0.5), there are two critical values of η_0—say, $\bar{\eta}_0$ and η_0^*—such that $\lim_{\alpha\downarrow 0}\eta_0=\bar{\eta}_0$ and $\lim_{\alpha\uparrow\infty}\eta_0=\eta_0^*$. These are given by the zeros of the numerator and the denominator of Eq. (3.3); namely, $\bar{\eta}_0$ is given by $1/2-v_i(\bar{\eta}_0)-a_0=0$ and $\eta_0^*=-\sqrt{d}/2\ln(1-2s_0)$, respectively [Figs. 14(a) and 14(b)]. However, for large s_0 (>0.5), $\eta_0=\infty$ as α tends to $\alpha_\infty=\lim_{\eta_0\uparrow\infty}\alpha=[2\hat{a}_0+\ln(2\mu+1)]/(2s_0-1)$ [Fig. 14(c)].

Similarly, the existence of standing spot solutions can be shown, as displayed in Fig. 15. The dependence of η_0 on α and s_0 is qualitatively similar to the one-dimensional problem; η_0^* is replaced by the root of $(\eta_0/\sqrt{d})I_1(\eta_0/\sqrt{d})K_0(\eta_0/\sqrt{d})-s_0=0$.

IV. STABILITY OF RADIALLY SYMMETRIC EQUILIBRIUM SOLUTIONS

In this section, we discuss the stability of the radially symmetric equilibrium solutions $(\eta_0,\ \bar{v}(r),\ \bar{w}(r))$ obtained in the previous section. In order to do so, we study the distribution of the eigenvalues of the linearized equations (2.1)–(2.8) around $(\eta_0,\ \bar{v}(r),\ \bar{w}(r))$, following the procedure used in Ref. [12]. Since the derivation of the stability formula is similar to the one in Ref. [33], we only show its final formula and some stability results.

A. One-dimensional problem

For a suitably large d, we take α, σ, and τ as free parameters. The exponential growth of perturbations to the standing pulse solution $(\eta_0,\ \bar{v}(x),\ \bar{w}(x))$, which is symmetric at $x=0$, is determined by the roots of the following equation:

$$\begin{aligned}F_\pm(z;d,\alpha,\sigma,\tau)\equiv -z-\frac{4}{\sigma}\Bigg[&\frac{-\mu}{2\sqrt{1+\mu}}(1-e^{-2\sqrt{1+\mu}\eta_0})\\&+\frac{\mu}{2\sqrt{1+\mu+z}}(1\pm e^{-2\sqrt{1+\mu+z}\eta_0})\\&+\left(\frac{\partial a}{\partial w}\right)_0\left\{\frac{-1}{2\sqrt{d}}(1-e^{-2\eta_0/\sqrt{d}})\right.\\&\left.+\frac{1}{2\sqrt{d(1+\tau z)}}(1\pm e^{-2\sqrt{(1+\tau z)/d}\eta_0})\right\}\Bigg]=0,\end{aligned} \tag{4.1}$$

with

$$\left(\frac{\partial a}{\partial w}\right)_0=\frac{\alpha}{2}\frac{1}{\cosh^2(\alpha\bar{w}_i+a_0)}, \tag{4.2}$$

where η_0 is obtained by the function $\alpha=\alpha(\eta_0)$, as shown in Fig. 14. We simply write $F_\pm(z;d,\alpha,\sigma,\tau)$ as $F_\pm(z)$, where

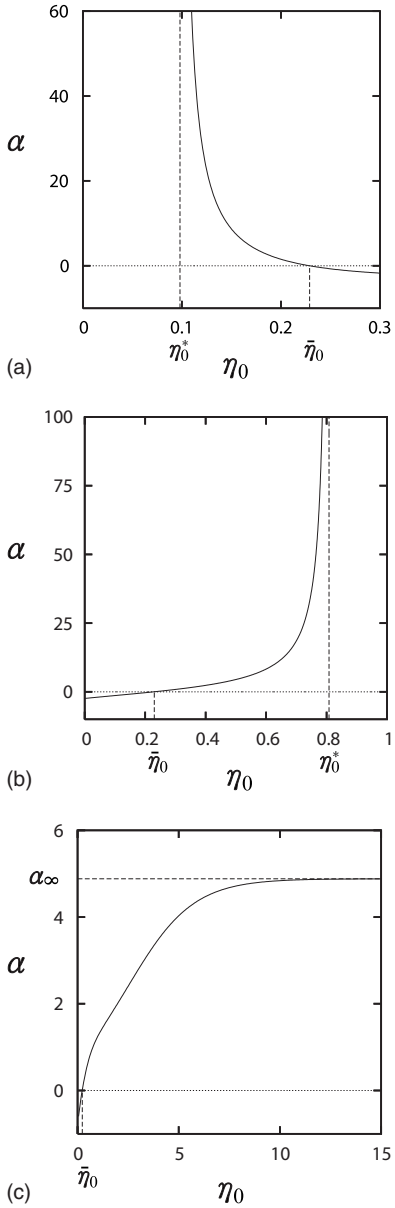

FIG. 14. α-η_0 relation of standing pulses of Eq. (3.3) ($d=10.0$). (a) s_0 is small ($s_0=0.03$). (b) s_0 is large ($s_0=0.2$). (c) s_0 is extremely large ($s_0=0.6$).

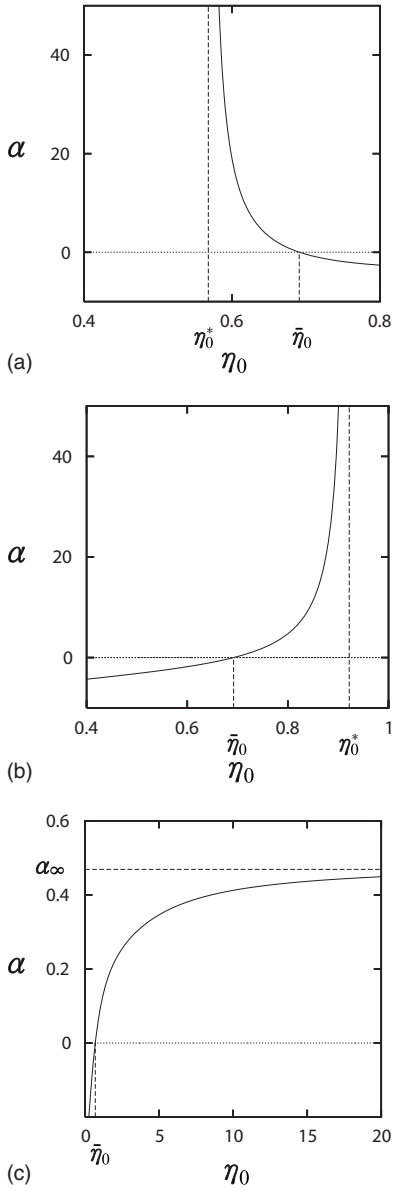

FIG. 15. α-η_0 relation of standing spots of Eq. (3.3) ($d=10.0$). (a) s_0 is small ($s_0=0.03$). (b) s_0 is large ($s_0=0.06$). (c) s_0 is extremely large ($s_0=1.5$).

$F_+(z)$ and $F_-(z)$ correspond to the cases of symmetric and antisymmetric perturbations, respectively. It is obvious that $F_-(0)=0$ holds for any $\sigma>0$; this implies the translational invariance. If $F_-(z)=0$ is doubly degenerated at $z=0$, that is,

$$F_-(0) = \frac{dF_-(0)}{dz} = 0, \tag{4.3}$$

it implies the occurrence of translational instability. Equation (4.1) with Eq. (4.3) gives the following relation between σ and α:

$$\sigma = \sigma_t(\alpha;\tau) = -\frac{2\mu}{(1+\mu)^{3/2}}\left\{-\frac{(1-e^{-2\sqrt{1+\mu}\eta_0})}{2} + (1+\mu)^{1/2}\eta_0 e^{-2\sqrt{1+\mu}\eta_0}\right\} - 2\left(\frac{\tau}{d}\right)\left(\frac{\partial a}{\partial w}\right)_0\left\{\frac{-1}{2}\sqrt{d}(1-e^{-2\eta_0/\sqrt{d}}) + \eta_0 e^{-2\eta_0/\sqrt{d}}\right\}. \tag{4.4}$$

The above equation suggests that $\sigma_t(\alpha;\tau)$ is determined by the first term when τ is small and d is large in the present case.

On the other hand, if $F_+(z)=0$ has a pair of pure imaginary solutions $\pm ki$ for some real k, it gives the relation be-

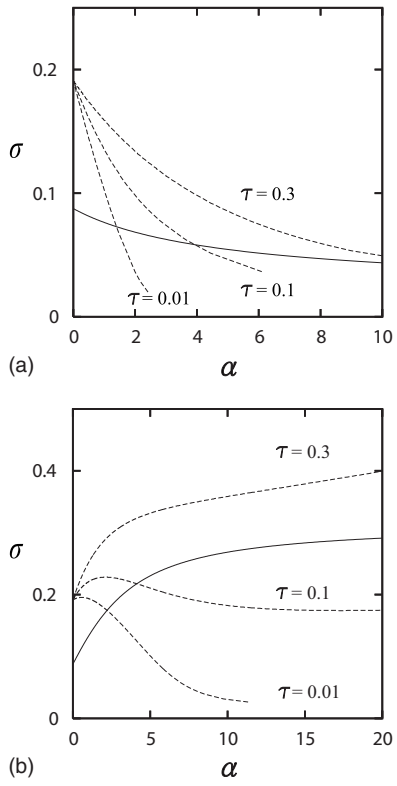

FIG. 16. Bifurcation diagram obtained by the linear stability analysis of the standing pulses to the interface equations (2.1)–(2.8). The solid and dashed curves, respectively, represent $\sigma=\sigma_t(\alpha;\tau)$ and $\sigma=\sigma_o(\alpha;\tau)$. For $\sigma_t(\alpha;\tau)$, the case $\tau=0.01$ is shown ($d=10.0$). (a) s_0 is small ($s_0=0.03$). (b) s_0 is large ($s_0=0.2$).

tween σ and α—say, $\sigma=\sigma_o(\alpha;\tau)$. It implies the occurrence of oscillatory instability. We can now draw the bifurcation diagram on the stability of $(\eta_0, \bar{v}(x), \bar{w}(x))$ in the (α,σ)-plane for different values of τ, as shown in Fig. 16. As $\sigma_t(\alpha;\tau)$ depends weakly on τ, $\sigma_t(\alpha;\tau)$ is drawn for $\tau=0.01$. We note that for small τ, the bifurcation curves $\sigma_t(\alpha;\tau)$ and $\sigma_o(\alpha;\tau)$ intersect at one point in the (α,σ)-plane, while for large τ, $\sigma_o(\alpha;\tau)$ is above $\sigma_t(\alpha;\tau)$ for any α. This diagram indicates the following properties: let τ be small. When α is small, the standing pulse is stable for large σ, while as σ decreases, it is primarily destabilized through oscillatory bifurcation. However, when α is large, as σ decreases, the standing pulse is primarily destabilized through translational bifurcation. On the other hand, let τ be large. The standing pulse is always destabilized through oscillatory bifurcation as σ decreases.

B. Traveling pulse solution

In the previous subsection, for suitable s_0, τ, d, and α, the occurrence of translational bifurcation suggests the appearance of the traveling pulses of Eqs. (1.6)–(1.9). A traveling pulse of the limiting problem derived from Eqs. (2.1)–(2.8) is of the form $(z_+-z_-,v_0(z),w_0(z))$ with $z=x-ct$, where c is the traveling speed and $z_\pm$ $(z_+>z_-)$ are the positions of the interfaces. Then, Eqs. (2.5) and (2.6) become

$$0=v_{zz}+cv_z+\mu[H(z-z_-)H(-z+z_+)-v]-v, \quad (4.5)$$

with boundary conditions

$$v(z=z_\pm-0)=v(z=z_\pm+0),$$

$$v_z(z=z_\pm-0)=v_z(z=z_\pm+0),$$

$$\lim_{|z|\to\infty} v(z)=0, \quad (4.6)$$

and Eqs. (2.7) and (2.8) become

$$0=dw_{zz}+\tau cw_z+H(z-z_-)H(-z+z_+)-w-s_0, \quad (4.7)$$

with boundary conditions

$$w(z=z_\pm-0)=w(z=z_\pm+0),$$

$$w_z(z=z_\pm-0)=w_z(z=z_\pm+0),$$

$$\lim_{|z|\to\infty} w(z)=-s_0. \quad (4.8)$$

The solution $(u_0(z),v_0(z),w_0(z))$ of Eqs. (4.5)–(4.8) is given as follows:

$$u_0(z)=\begin{cases} -C_1e^{\lambda_v^+z}, & -\infty<z<z_-,\\ -C_2e^{\lambda_v^-z}-C_3e^{\lambda_v^+z}+\dfrac{1}{\mu+1}, & z_-<z<z_+,\\ -C_4e^{\lambda_v^-z}, & z_+<z<\infty, \end{cases} \quad (4.9)$$

$$v_0(z)=\begin{cases} C_1e^{\lambda_v^+z}, & -\infty<z<z_-,\\ C_2e^{\lambda_v^-z}+C_3e^{\lambda_v^+z}+\dfrac{\mu}{\mu+1}, & z_-<z<z_+,\\ C_4e^{\lambda_v^-z}, & z_+<z<\infty, \end{cases} \quad (4.10)$$

and

$$w_0(z)=\begin{cases} D_1e^{\lambda_w^+z}-s_0, & -\infty<z<z_-,\\ D_2e^{\lambda_w^-z}+D_3e^{\lambda_w^+z}+1-s_0, & z_-<z<z_+,\\ D_4e^{\lambda_w^-z}-s_0, & z_+<z<\infty. \end{cases} \quad (4.11)$$

Here, $\lambda_{v,\pm}$ and $\lambda_{w,\pm}$ are, respectively,

$$\lambda_v^\pm=\frac{1}{2}[-c\pm\sqrt{c^2+4(\mu+1)}],$$

$$\lambda_w^\pm=\frac{1}{2d}[-\tau c\pm\sqrt{(\tau c)^2+4d}], \quad (4.12)$$

and the coefficients C_i and D_i $(i=1,2,3,4)$ are given as follows:

$$C_1=\left(\frac{\mu}{\mu+1}\right)\left(\frac{\lambda_v^-}{\lambda_v^+-\lambda_v^-}\right)(e^{-\lambda_v^+z_+}-e^{-\lambda_v^+z_-}),$$

$$C_2 = -\left(\frac{\mu}{\mu+1}\right)\left(\frac{\lambda_v^+}{\lambda_v^+ - \lambda_v^-}\right)e^{-\lambda_v^- z_-},$$

$$C_3 = \left(\frac{\mu}{\mu+1}\right)\left(\frac{\lambda_v^-}{\lambda_v^+ - \lambda_v^-}\right)e^{-\lambda_v^+ z_+},$$

$$C_4 = \left(\frac{\mu}{\mu+1}\right)\left(\frac{\lambda_v^+}{\lambda_v^+ - \lambda_v^-}\right)(e^{-\lambda_v^- z_+} - e^{-\lambda_v^- z_-}), \tag{4.13}$$

and

$$D_1 = \left(\frac{\lambda_w^-}{\lambda_w^+ - \lambda_w^-}\right)(e^{-\lambda_w^+ z_+} - e^{-\lambda_w^+ z_-}),$$

$$D_2 = -\left(\frac{\lambda_w^+}{\lambda_w^+ - \lambda_w^-}\right)e^{-\lambda_w^- z_-},$$

$$D_3 = \left(\frac{\lambda_w^-}{\lambda_w^+ - \lambda_w^-}\right)e^{-\lambda_w^+ z_+},$$

$$D_4 = \left(\frac{\lambda_w^+}{\lambda_w^+ - \lambda_w^-}\right)(e^{-\lambda_w^- z_+} - e^{-\lambda_w^- z_-}). \tag{4.14}$$

Using Eq. (2.1), the set $(\sigma, c, z_+ - z_-)$ can be determined by the condition

$$-\left(\frac{d\Gamma(t)}{dt}\cdot\nu\right)_{z=z_-} = \left(\frac{d\Gamma(t)}{dt}\cdot\nu\right)_{z=z_+} = c. \tag{4.15}$$

The dependences of speed c on σ and pulse width $l=(z_+ - z_-)$ have already been shown in Fig. 8. We thus find that traveling pulse solutions bifurcate from the standing ones as σ decreases. Here, we make two observations: (i) the bifurcation is subcritical for the case $\alpha=0$, while it is supercritical for large α, and (ii) as the speed c increases, λ_v^+ becomes small, while $\lambda_v^- \approx -c$, so that $v(z_-)$ remains to take a certain value, while $v(z_+)$ becomes vanishingly small. This implies that the profile of v is asymmetric around the center of the pulse for large c. On the contrary, even if c is large, when τ is small and d is large, we know $\lambda_w^+ \approx -\lambda_w^- = 1/\sqrt{d}$, so that $w(z_+)$ and $w(z_-)$ are almost the same. This indicates that the profile of w is rather symmetric around the center of the pulse.

C. Two-dimensional problem

Next, we discuss the stability of the standing spot solutions $(\eta_0, \bar{v}(r), \bar{w}(r))$. Suppose that small perturbations with $2\pi/n$ periodic deformations of the radial direction $(n=0,1,2,\ldots)$ are introduced into them. Then, the stability formula corresponding to Eq. (4.1) is given by

$$F_n(z;d,\alpha,\sigma,\tau) = -\sigma z + \frac{\epsilon}{\eta_0^2}(1-n^2) + \Gamma_v - \hat{\phi}_n^{(v)}(z) + \Gamma_w - \hat{\phi}_n^{(w)}(z), \tag{4.16}$$

with

$$\Gamma_v = 4\eta_0\mu I_1(\sqrt{1+\mu}\,\eta_0)K_1(\sqrt{1+\mu}\,\eta_0), \tag{4.17}$$

$$\hat{\phi}_n^{(v)}(z) = 4\eta_0\mu I_n(\sqrt{1+\mu+z}\,\eta_0)K_n(\sqrt{1+\mu+z}\,\eta_0), \tag{4.18}$$

$$\Gamma_w = 4\left(\frac{\partial a}{\partial w}\right)_0\left(\frac{\eta_0}{d}\right)I_1(\eta_0/\sqrt{d})K_1(\eta_0/\sqrt{d}), \tag{4.19}$$

and

$$\hat{\phi}_n^{(w)}(z) = 4\left(\frac{\partial a}{\partial w}\right)_0\left(\frac{\eta_0}{d}\right)I_n\left(\sqrt{\frac{1+\tau z}{d}}\,\eta_0\right)K_n\left(\sqrt{\frac{1+\tau z}{d}}\,\eta_0\right), \tag{4.20}$$

where I_n and K_n are the modified Bessel functions. It is obvious that $F_1(0)=0$ for any $\sigma>0$, which corresponds to the translational invariance. In a manner similar to the one-dimensional case, we consider the situation where $F_1(z)$ is doubly degenerated at $z=0$—that is,

$$F_1(0) = \frac{dF_1(0)}{dz} = 0, \tag{4.21}$$

giving the relation between α and σ as

$$\begin{aligned}\sigma = \sigma_{1,t}(\alpha;\tau) = &-\frac{\mu\eta_0^2}{\sqrt{1+\mu}}\{K_1(\sqrt{1+\mu}\,\eta_0)[I_0(\sqrt{1+\mu}\,\eta_0) + I_2(\sqrt{1+\mu}\,\eta_0)] - I_1(\sqrt{1+\mu}\,\eta_0)[K_0(\sqrt{1+\mu}\,\eta_0) \\ &+ K_2(\sqrt{1+\mu}\,\eta_0)]\} - \left(\frac{\partial a}{\partial w}\right)_0\frac{\eta_0^2\tau}{d^{3/2}}\{K_1(\eta_0/\sqrt{d})[I_0(\eta_0/\sqrt{d}) \\ &+ I_2(\eta_0/\sqrt{d})] - I_1(\eta_0/\sqrt{d})[K_0(\eta_0/\sqrt{d}) + K_2(\eta_0/\sqrt{d})]\}.\end{aligned} \tag{4.22}$$

Similar to $\sigma_t(\alpha;\tau)$ in the one-dimensional case, $\sigma_{1,t}(\alpha;\tau)$ depends weakly on the second term as long as d is large and τ is small in the present case. The static bifurcation $\sigma=\sigma_{n,s}(\alpha;\tau)$ $(n=2,3,\ldots)$ and the oscillatory one $\sigma=\sigma_{0,o}(\alpha;\tau)$ are obtained, respectively, by $F_n(0)=0$ and $F_0(ik)=0$ for some real k. The bifurcation diagram of the standing spot solution is shown in the (α,σ)-plane in Fig. 17. As $\sigma_{1,t}(\alpha;\tau)$ and $\sigma_{2,s}(\alpha;\tau)$ depend weakly on τ, $\sigma_{1,t}(\alpha;\tau)$ and $\sigma_{2,s}(\alpha;\tau)$ are drawn for $\tau=0.01$. Regardless of s_0, when α is increased over the critical value $\alpha_{2,s}$, the standing spot solution is primarily destabilized through the static bifurcation with $n=2$ mode.

First, we consider the case where s_0 is small, as shown in Fig. 17(a). In the region $\alpha \le \alpha_{2,s}$, when α is small, the standing spot solution is primarily destabilized through oscillatory bifurcation for any value of τ. However, when α is large and τ is small, the standing spot solution is primarily destabilized through the translational bifurcation. This implies that the second inhibitor suppresses the oscillatory bifurcation and enhances the translational motion of the spot. As shown in Fig. 11(a), when τ and σ are small and d is large, taking suitable α, traveling spots appear as a result of the synergistic effect of two inhibitors on one activator. If α is sufficiently large satisfying $\alpha \ge \alpha_{2,s}$, the bifurcation diagram sug-

gests that the standing spot solution is primarily destabilized through the static bifurcation with $n=2$ mode and there is no traveling spot solution. We can see by the numerical simulation that a single spot splits into many spots, as shown in Fig. 11(b).

In contrast, for a larger value of s_0, we note that $\alpha_{2,s}$ is smaller than that for the case of a small value of s_0 [Fig. 17(b)]. For $\alpha \leq \alpha_{s,2}$, the bifurcation curve $\sigma=\sigma_{0,o}(\alpha;\tau)$ is higher than $\sigma=\sigma_{1,t}(\alpha;\tau)$ for any value of τ. Then, the standing spot is destabilized through the oscillatory bifurcation by decreasing σ. However, for large α satisfying $\alpha \geq \alpha_{2,s}$, the standing spot solution is destabilized through the static bifurcation with $n=2$ mode. Thus, for a larger value of s_0, the lateral inhibition by the second inhibitor does not yield a traveling spot solution, but causes the splitting of a standing spot.

V. REDUCED SYSTEMS OF THE THREE-COMPONENT RD SYSTEM

We first consider the limits $\tau \to 0$ and $d \to \infty$. In this case, w is a time-dependent but spatially independent variable, given by

$$w(t) = \frac{1}{|\Omega|}\int_{R^n} (u+v)d\mathbf{x} - s_0 = |\Omega_1(t)| - s_0, \qquad (5.1)$$

where the spatial coordinate is rescaled to absorb $|\Omega|$ in the integration and $|\Omega_1(t)|$ is a measure of $\Omega_1(t)$. Then, the three-component RD system (1.6)–(1.8) with Eq. (1.9) is reduced to a two-component RD system with a global inhibitory coupling term:

$$\epsilon\sigma u_t = \epsilon^2\nabla^2 u + H[u-a(t)] - u - v, \qquad (5.2)$$

$$t>0, \quad \mathbf{x} \in R^n,$$

$$v_t = \nabla^2 v + \mu u - v, \qquad (5.3)$$

where $a(t)$ is given as

$$a(t) = \frac{1}{2}(1+\tanh\{\alpha[|\Omega_1(t)| - s_0] + \hat{a}_0\}). \qquad (5.4)$$

Systems similar to the one given above have been studied in Refs. [33,34]. The variation of $|\Omega_1(t)|$ is considered in these systems as a global feedback. Furthermore, we consider the limit $\alpha \to \infty$. For this case, $a(t)$ changes under a constraint

$$|\Omega_1(t)| = s_0. \qquad (5.5)$$

That is, an area enclosed by an interface $\Gamma(t)$ is conserved. Thus, in the limits $\tau \to 0$, $d \to \infty$, and $\alpha \to \infty$, the three-component RD system (1.6)–(1.8) with Eq. (1.9) is reduced to a two-component RD system with area conservation.

We consider the system (5.2) and (5.3), where $a(t)$ is determined under the constraint (5.5). In this limiting case, the radius of the core is given as $\eta_0=\eta_0^*$. The stability of the solution $(\eta_0^*, \bar{v}(r), \bar{w}(r))$ is obtained in the same manner as that in the previous section. Here, we choose s_0 and σ as free parameters. Under the constraint (5.5), the oscillatory bifurcation is completely suppressed for one- and two-dimensional solutions. In one dimension, as σ decreases, the standing pulse is destabilized through translational bifurcation [Fig. 18(a)]. On the other hand, in two dimensions, there is one critical s_0^*. When $s_0 \leq s_0^*$, the standing spot is primarily destabilized through the translational bifurcation with decreasing σ. However, when $s_0 \geq s_0^*$, the standing spot is destabilized through the static bifurcation with $n=2$ mode. Thus, in this limiting case, the traveling spots exist for $s_0 \leq s_0^*$.

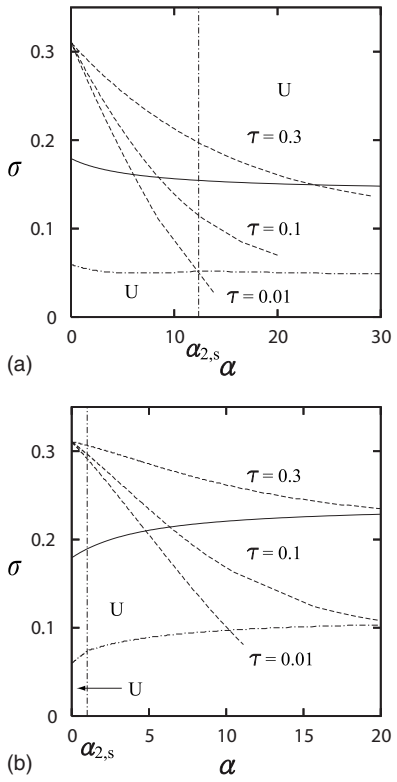

FIG. 17. Bifurcation diagram obtained by the linear stability analysis of the standing spots to the interface equations (2.1)–(2.8). The solid, dashed, and dash-dotted curves, respectively, represent $\sigma=\sigma_{1,t}(\alpha;\tau)$, $\sigma=\sigma_{0,o}(\alpha;\tau)$, and $\sigma=\sigma_{2,s}(\alpha;\tau)$. For $\sigma_{1,t}(\alpha;\tau)$ and $\sigma_{2,s}(\alpha;\tau)$, the case $\tau=0.01$ is shown. The mark U in the figures denotes the unstable region of the static bifurcation with $n=2$ mode ($d=10.0$). (a) s_0 is small ($s_0=0.03$). (b) s_0 is large ($s_0=0.06$).

VI. TRANSVERSAL STABILITY OF TRAVELING PULSE SOLUTIONS

As shown in Sec. I C, we observe that planar traveling pulse solutions of Eqs. (1.6)–(1.9) with small τ and large d are transversally destabilized when α is large. We discuss the stability of these solutions by using the singular perturbation method.

Let us consider planar traveling pulse solutions $(u(z),v(z),w(z))$ $(z=x-ct)$ in a domain $\Omega=\{(z,y)\in R^2 | z\in R, \ y\in R\}$. These are equilibrium solutions of the following system:

$$\epsilon\sigma u_t = \epsilon^2(u_{zz}+u_{yy}) + \epsilon\sigma c u_z + H[u-a(w)] - u - v, \qquad (6.1)$$

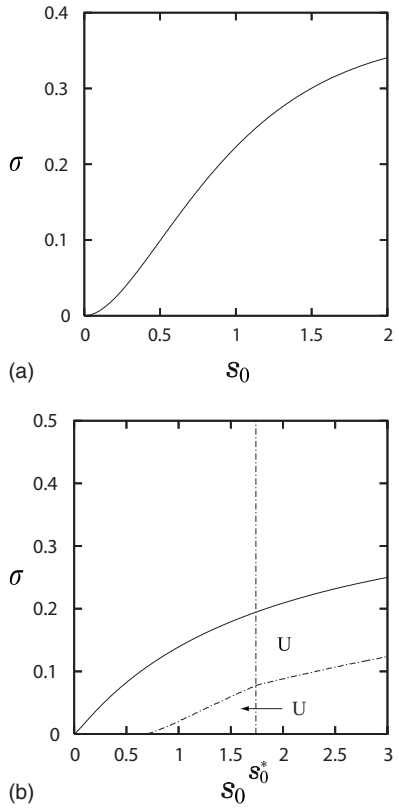

FIG. 18. Bifurcation diagram obtained by the linear stability analysis of the standing pulses and spots to the interface equations (2.1)–(2.8) in the limits $\tau \to 0$, $d \to \infty$, and $\alpha \to \infty$. The mark U in the figure denotes the unstable region of the static bifurcation with $n=2$ mode. (a) One-dimensional case. The solid line represents $\sigma_t(s_0)$. (b) Two-dimensional case. The solid and dash-dotted curves, respectively, represent $\sigma=\sigma_{1,t}(s_0)$ and $\sigma=\sigma_{2,s}(s_0)$.

$$v_t = (v_{zz} + v_{yy}) + cv_z + \mu u - v, \quad t > 0, \quad (z,y) \in \Omega, \tag{6.2}$$

$$\tau w_t = d(w_{zz} + w_{yy}) + \tau c w_z + u + v - w - s_0, \tag{6.3}$$

with

$$a(w) = \frac{1}{2}[1 + \tanh(\alpha w + \hat{a}_0)]. \tag{6.4}$$

The boundary conditions are

$$\lim_{|z| \to \infty} (u,v,w) = (0,0,-s_0) \tag{6.5}$$

and

$$\lim_{|y| \to \infty} \left(\frac{\partial u}{\partial y}, \frac{\partial v}{\partial y}, \frac{\partial w}{\partial y} \right) = (0,0,0). \tag{6.6}$$

The detailed derivation of the stability formula is given in the Appendix; here, we only show the final results and the related bifurcation diagrams.

Assuming suitable s_0, d, α, σ, and τ, the exponential growth of perturbations with wave number k is determined by the roots of the following equation:

$$F(s,k) = \det(A) = a_{11}a_{22} - a_{12}a_{21} = 0. \tag{6.7}$$

Here, a_{ij} $(i,j=1,2)$ are given as follows:

$$a_{11} = -\sigma s - \epsilon k^2 + \mu \left(\frac{\partial C}{\partial v} \right)_0 \left[\frac{1}{p_1}(e^{\lambda_v^- l} - 1) + \frac{1}{2p_2} \right] + \left(\frac{\partial C}{\partial a} \right)_0 \left(\frac{\partial a}{\partial w} \right)_0^+ \left[\frac{1}{p_3}(e^{\lambda_w^- l} - 1) + \frac{1}{2p_4} \right],$$

$$a_{12} = \left(\frac{\partial C}{\partial v} \right)_0 \frac{\mu}{2} \left[-\frac{1}{p_2} e^{-(p_2 + c/2)l} \right] - \left(\frac{\partial C}{\partial a} \right)_0 \left(\frac{\partial a}{\partial w} \right)_0^+ \frac{1}{2} \left[\frac{1}{p_4} e^{-(p_4/d + \tau c/2d)l} \right],$$

$$a_{21} = \left(\frac{\partial C}{\partial v} \right)_0 \frac{\mu}{2} \left[-\frac{1}{p_2} e^{-(p_2 - c/2)l} \right] - \left(\frac{\partial C}{\partial a} \right)_0 \left(\frac{\partial a}{\partial w} \right)_0^- \frac{1}{2} \left[\frac{1}{p_4} e^{-(p_4/d - \tau c/2d)l} \right],$$

$$a_{22} = -\sigma s - \epsilon k^2 + \mu \left(\frac{\partial C}{\partial v} \right)_0 \left[\frac{1}{p_1}(e^{-\lambda_v^+ l} - 1) + \frac{1}{2p_2} \right] + \left(\frac{\partial C}{\partial a} \right)_0 \left(\frac{\partial a}{\partial w} \right)_0^- \left[\frac{1}{p_3}(e^{-\lambda_w^+ l} - 1) + \frac{1}{2p_4} \right], \tag{6.8}$$

with

$$l = (z_+ - z_-),$$

$$p_1 = \sqrt{c^2 + 4(\mu + 1)},$$

$$p_2 = \sqrt{k^2 + \frac{c^2}{4} + (\mu + 1) + s},$$

$$p_3 = \sqrt{(c\tau)^2 + 4d},$$

$$p_4 = \sqrt{(dk)^2 + \frac{(c\tau)^2}{4} + d + \tau d s}, \tag{6.9}$$

$$\left(\frac{\partial C}{\partial a} \right)_0 = \left(\frac{\partial C}{\partial v} \right)_0 = -\frac{1}{2\sigma}[4 + (c\sigma)^2]^{3/2}, \tag{6.10}$$

and

$$\left(\frac{\partial a}{\partial w} \right)_0^{\pm} = \frac{\alpha}{2} \frac{1}{\cosh^2[\alpha w(z = z_\pm) + \hat{a}_0]}. \tag{6.11}$$

It is obvious that $F(0,0)=0$; this corresponds to the translational invariant mode. The bifurcation threshold is determined by substituting $s=0$ in Eq. (6.7). When $\alpha=0$, there is no other solution, suggesting that the traveling pulse solution is transversally stable for perturbations. On the other hand, for $\alpha>0$, there are other branches, as shown in Figs. 19(a) and 19(b), depending on ϵ. For the limit $\epsilon \downarrow 0$, we observe that there are two branches that diverge as $\sim \epsilon^{-1/2}$ and another branch is independent of ϵ. The bifurcation diagrams

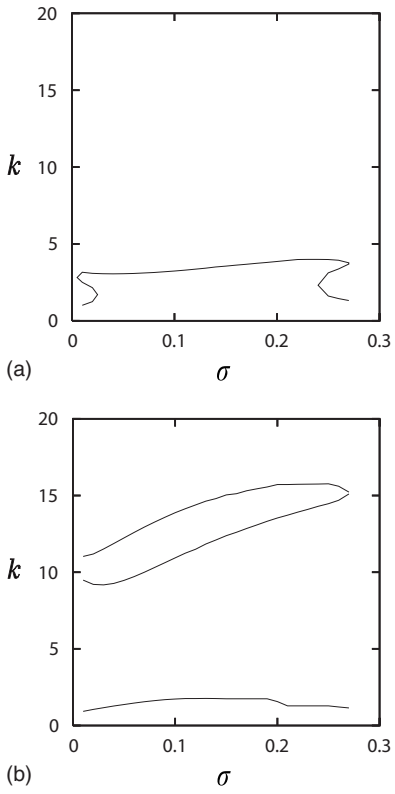

FIG. 19. Bifurcation diagram of planar traveling pulses in the (σ, k)-plane ($d=10.0$, $\tau=0.01$, $\alpha=10.0$, and $s_0=0.2$). (a) $\epsilon=1.25\times10^{-1}$. (b) $\epsilon=1.25\times10^{-2}$.

suggest that when d is large and τ is small, the traveling pulse solution is transversally destabilized through the lateral inhibition of w as α increases.

Let us consider the system in the channel domain $\Omega_L=\{\mathbf{x}=(x,y)\in R^2 | x\in R,\ 0<y<L\}$ with the Neumann boundary conditions on $y=0$ and $y=L$. Taking $k=\pi n/L$ with integer n, the above bifurcation diagrams indicate that the traveling pulses are transversally unstable in the limit $\epsilon\downarrow 0$. On the other hand, for finite ϵ, the traveling pulses are unstable if the system size L is sufficiently large to include components of a destabilizing wave number.

VII. CONCLUDING REMARKS

We have studied a three-component RD system with one activator and two inhibitors. The main advantage of our system is the mathematical tractability. It results from the replacement of the common cubic nonlinearity by a piecewise linear function in Eq. (1.6). Traveling spots have already been reported in Refs. [23,26], where the cubic nonlinearity was applied. Although there is no qualitative difference in the phenomenon, the stability analysis of the standing pulse (spot) solution by the singular perturbation procedures is difficult in them.

We have found that the synergistic effect of the slow and short-range inhibitor v, the *traveling pulse generator*, and the fast and long-range one w, the *lateral inhibition localizer*, induces several remarkable phenomena in the traveling pulse and spot dynamics of the solutions. With regard to the traveling pulses, the distribution of v is asymmetric around the center of the pulse, while that of w is almost symmetric. This suggests that the intrinsic traveling speed depends mostly on the difference of v between the front and back layers. However, w plays important roles in the nonannihilation of traveling pulses and in the suppression of the expanding wave to generate a traveling spot. In one dimension, the oscillatory bifurcation is suppressed and the standing pulse bifurcates to a traveling pulse with decreasing σ. Fast traveling pulses collide elastically under a strong repulsive force due to w. It is shown that slow traveling pulses in two-component RD system collide elastically; this mechanism is analyzed using the perturbation theory under the assumption that the deformation of the traveling pulse from the standing one is small [32]. In contrast, in our three-component RD system, the deformation on collision is large, and thus the perturbation theory is not applicable. Fast traveling pulses collide elastically; however, slow traveling pulses cannot approach closely and stop before collision. This is one of the remarkable properties of our three-component RD system. In two dimensions, w suppresses the oscillatory and the static bifurcation with $n=2$ mode, and a traveling spot bifurcates from a standing spot with decreasing σ. For a stable traveling spot, large d and small τ are necessary. It suggests that a fast and long-range w suppresses the expansion of the spot. s_0 determines the radius of the standing spot. For small s_0, although a stable traveling spot exists in some range of α, an extremely large α causes a splitting of the spot. In contrast, for large s_0, the standing spot with a large radius is destabilized through the static bifurcation with $n=2$ mode with decreasing σ. It is understood that w causes a lateral inhibition, leading to the splitting of the spot. Similarly, a planar traveling pulse is destabilized through the lateral inhibition.

In the limits $\tau\to 0$, $d\to\infty$, and $\alpha\to\infty$, the three-component RD system is reduced to a two-component RD system with area conservation. In one dimension, the oscillatory bifurcation is completely suppressed and a standing pulse bifurcates to a traveling pulse with decreasing σ. In two dimensions, although there is no oscillatory bifurcation, the traveling spot exists only for smaller s_0 due to the static bifurcation with $n=2$ mode. For finite α, $|\Omega_1(t)|$ is a time-dependent variable and our RD system is reduced to a two-component RD system with a global inhibitory coupling term. Similar systems have been studied, and the appearance of the elastic and inelastic collisions of traveling spots has been observed [33,34]. The interaction of traveling spots in a three-component RD system has been studied in Refs. [25,26,35]. Slow traveling spots collide elastically; however, fast traveling spots fuse and split into two spots on collision. For small τ, large d, and finite α in our system, these interesting phenomena are expected. The study of the interaction between traveling spots is reported elsewhere.

ACKNOWLEDGMENTS

The authors would like to thank T. Ohta for his valuable discussions on the interface-dynamics approach used in this paper. M.M. is grateful to a Grant-in-Aid for Scientific Research No. (S) 18104002 for its support.

APPENDIX

Following the procedure used in Ref. [12], the stability formula $F(s,k)=0$, given in Sec. VI, can be derived. We briefly show their derivations.

Let $(u_0(z,y),v_0(z,y),w_0(z,y))$ be the two-dimensional equilibrium solution of Eqs. (6.1)–(6.4). Let $\zeta^{\pm}(y,0)$ be small disturbances on the stationary interface $z=z_{\pm}$ at $t=0$ and $\zeta^{\pm}(y,t)$ be the corresponding deviations from $z=z_{\pm}$ such that the resulting interfaces are

$$z_{\pm}^{I}(t)=z_{\pm}+\zeta^{\pm}. \tag{A1}$$

The equation of the interfaces is given by

$$\sigma V_n = \pm C(v_I;a(w_I))-\epsilon\kappa, \tag{A2}$$

where V_n and κ are the normal component of velocity and curvature of the interface, respectively.

We write the values of v and w on the interface as $v_I^{\pm}(\zeta,t)=v(z_{\pm}+\zeta^{\pm}(y,t),y)$ and $w_I^{\pm}(\zeta,t)=w(z_{\pm}+\zeta^{\pm}(y,t),y)$, respectively, and expand them in powers of $\zeta^{\pm}(y,t)$ up to $O(\zeta^{\pm})$ as follows:

$$v_I^{\pm}(y,t)=v_0^{\pm}+v_1^{\pm}(y,t)+v_2^{\pm}(y,t),$$

$$w_I^{\pm}(y,t)=w_0^{\pm}+w_1^{\pm}(y,t)+w_2^{\pm}(y,t), \tag{A3}$$

where

$$v_0^{\pm}=\pm\left(\frac{\mu}{\mu+1}\right)\frac{\lambda_v^{\pm}}{p_1}[1-e^{\pm\lambda_v^{\mp}l}]=\bar{v}_i^{\pm},$$

$$v_1^{\pm}(y,t)=\pm\frac{\mu}{p_1}[e^{\pm\lambda_v^{\mp}l}-1]\zeta^{\pm}(y,t),$$

$$v_2^{\pm}(y,t)=\frac{1}{(2\pi)^2}\int e^{-iq_yy}e^{-iq_zz_{\pm}}d\mathbf{q}\times\int_0^t e^{-[|\mathbf{q}|^2+icq_z+\mu+1]t'}dt'\mu\int[e^{iq_zz_+}\zeta^{+}(y',t-t')-e^{iq_zz_-}\zeta^{-}(y',t-t')]e^{iq_yy'}dy' \tag{A4}$$

and

$$w_0^{\pm}=\pm\frac{d\lambda_w^{\pm}}{p_3}[1-e^{\pm\lambda_w^{\mp}l}]-s_0=\bar{w}_i^{\pm},$$

$$w_1^{\pm}(y,t)=\pm\frac{\mu}{p_3}[e^{\pm\lambda_w^{\mp}l}-1]\zeta^{\pm}(y,t),$$

$$w_2^{\pm}(y,t)=\frac{1}{(2\pi)^2}\times\int e^{-iq_yy}e^{-iq_zz_{\pm}}d\mathbf{q}\int_0^t e^{-[d|\mathbf{q}|^2/\tau+icq_z+1/\tau]t'}\times dt'\frac{1}{\tau}\int[e^{iq_zz_+}\zeta^{+}(y',t-t')-e^{iq_zz_-}\zeta^{-}(y',t-t')]e^{iq_yy'}dy', \tag{A5}$$

where $\bar{v}_i^{\pm}$ and $\bar{w}_i^{\pm}$ are the values of $v_0(z,y)$ and $w_0(z,y)$ on the interfaces $z=z_{\pm}$, respectively.

Here, we put

$$l=(z_+-z_-),$$

$$p_1=\sqrt{c^2+4(\mu+1)},$$

$$p_2=\sqrt{k^2+\frac{c^2}{4}+(\mu+1)+s},$$

$$p_3=\sqrt{(c\tau)^2+4d},$$

$$p_4=\sqrt{(dk)^2+\frac{(c\tau)^2}{4}+d+\tau ds}. \tag{A6}$$

We also expand a as

$$a=a_0^{*}+a_1^{\pm}(t), \tag{A7}$$

where $a_0^{*}=\bar{a}^{\pm}=1/2[1+\tanh(\alpha\bar{w}_i^{\pm}+\hat{a}_0)]$ and $a_1^{\pm}(t)$ is the deviation associated with the motion of interfaces, given by

$$a_1^{\pm}(t)=\left(\frac{\partial a}{\partial w}\right)_0^{\pm}(w_1^{\pm}+w_2^{\pm}), \tag{A8}$$

with

$$\left(\frac{\partial a}{\partial w}\right)_0^{\pm}=\frac{\alpha}{2}\frac{1}{\cosh^2(\alpha\bar{w}_i^{\pm}+\hat{a}_0)}. \tag{A9}$$

Consequently, the equations of $\zeta^{\pm}(y,t)$ up to $O(\zeta^{\pm})$ are

$$\sigma\frac{d\zeta^{\pm}}{dt}=(\pm)\left(\frac{\partial C}{\partial v}\right)_0(v_1^{\pm}+v_2^{\pm})+(\pm)\left(\frac{\partial C}{\partial a}\right)_0 a_1+\epsilon\zeta_{yy}^{\pm}, \tag{A10}$$

where

$$\left(\frac{\partial C}{\partial v}\right)_0=\left(\frac{\partial C}{\partial v}\right)(\bar{v}_i^{\pm},a(\bar{w}_i^{\pm}))=\frac{-1}{2\sigma}[4+(c\sigma)^2]^{3/2}$$

and

$$\left(\frac{\partial C}{\partial a}\right)_0=\left(\frac{\partial C}{\partial a}\right)(\bar{v}_i^{\pm},a(\bar{w}_i^{\pm}))=\frac{-1}{2\sigma}[4+(c\sigma)^2]^{3/2}. \tag{A11}$$

Applying the Fourier transformation

$$\zeta_k^{\pm}(t)=\int\zeta^{\pm}(y,t)e^{+iky}dy \tag{A12}$$

to Eq. (A10), we have

$$\sigma\frac{d}{dt}\zeta_k^{\pm}=-\epsilon k^2\zeta_k^{\pm}(t)+(\pm)\left(\frac{\partial C}{\partial v}\right)_0(\tilde{v}_1^{\pm}+\tilde{v}_2^{\pm})+(\pm)\left(\frac{\partial C}{\partial a}\right)_0\left(\frac{\partial a}{\partial w}\right)_0^{\pm}(\tilde{w}_1^{\pm}+\tilde{w}_2^{\pm}), \tag{A13}$$

where

$$\tilde{v}_1^{\pm} = \pm \frac{\mu}{p_1}[e^{\pm\lambda_v^{\mp} l} - 1]\zeta_k^{\pm}(t),$$

$$\tilde{v}_2^{\pm} = \pm \frac{\mu}{2}\int_0^t \sqrt{\frac{1}{\pi t'}} e^{-[k^2+\mu+1]t'}[e^{-c^2 t'/4}\zeta_k^{\pm}(t-t') - e^{-(l \pm ct')^2/4t'}\zeta_k^{\mp}(t-t')]dt',$$

$$\tilde{w}_1^{\pm} = \pm \frac{\mu}{p_3}[e^{\pm\lambda_w^{\mp} l} - 1]\zeta_k^{\pm}(t),$$

$$\tilde{w}_2^{\pm} = \pm \frac{1}{2}\int_0^t \sqrt{\frac{1}{\pi\tau dt'}} e^{-[dk^2/\tau+1/\tau]t'}[e^{-\tau c^2 t'/4d}\zeta_k^{\pm}(t-t') - e^{-\pi'[c \pm l/t']^2/4d}\zeta_k^{\mp}(t-t')]dt'. \quad \text{(A14)}$$

We now apply the Laplace transformation

$$\hat{\zeta}_k^{\pm}(s) = \int_0^{\infty} \zeta_k^{\pm}(t)e^{-st}dt \quad \text{(A15)}$$

to Eq. (A13); we have

$$\sigma[s\hat{\zeta}_k^{\pm}(s) - \zeta_k^{\pm}(0)] = -\epsilon k^2 \hat{\zeta}_k^{\pm}(s) + (\pm)\left(\frac{\partial C}{\partial v}\right)_0 (\hat{v}_1^{\pm} + \hat{v}_2^{\pm}) + (\pm)\left(\frac{\partial C}{\partial a}\right)_0 \left(\frac{\partial a}{\partial w}\right)_0^{\pm} (\hat{w}_1^{\pm} + \hat{w}_2^{\pm}), \quad \text{(A16)}$$

where

$$\hat{v}_1^{\pm} = \pm \frac{\mu}{p_1}[e^{\pm\lambda_v^{\mp} l} - 1]\hat{\zeta}_k^{\pm},$$

$$\hat{v}_2^{\pm} = \pm \frac{\mu}{2p_2}[\hat{\zeta}_k^{\pm} - e^{-(p_2 \pm c/2)l}\hat{\zeta}_k^{\mp}],$$

$$\hat{w}_1^{\pm} = \pm \frac{1}{p_3}[e^{\pm\lambda_w^{\mp} l} - 1]\hat{\zeta}_k^{\pm},$$

$$\hat{w}_2^{\pm} = \pm \frac{1}{2p_4}[\hat{\zeta}_k^{\pm} - e^{-(p_4/d \pm \pi c/2d)l}\hat{\zeta}_k^{\mp}]. \quad \text{(A17)}$$

We can describe Eq. (A16) in the following matrix form:

$$\begin{pmatrix} -\sigma\zeta_k^{+}(0) \\ -\sigma\zeta_k^{-}(0) \end{pmatrix} = \begin{pmatrix} a_{11} & a_{12} \\ a_{21} & a_{22} \end{pmatrix}\begin{pmatrix} \hat{\zeta}_k^{+}(t) \\ \hat{\zeta}_k^{-}(t) \end{pmatrix} \equiv A\begin{pmatrix} \hat{\zeta}_k^{+}(t) \\ \hat{\zeta}_k^{-}(t) \end{pmatrix}, \quad \text{(A18)}$$

where $a_{ij}(i,j=1,2)$ are given as

$$a_{11} = -\sigma s - \epsilon k^2 + \mu\left(\frac{\partial C}{\partial v}\right)_0\left[\frac{1}{p_1}(e^{\lambda_v^{-} l} - 1) + \frac{1}{2p_2}\right] + \left(\frac{\partial C}{\partial a}\right)_0\left(\frac{\partial a}{\partial w}\right)_0^{+}\left[\frac{1}{p_3}(e^{\lambda_w^{-} l} - 1) + \frac{1}{2p_4}\right],$$

$$a_{12} = \left(\frac{\partial C}{\partial v}\right)_0 \frac{\mu}{2}\left[-\frac{1}{p_2}e^{-(p_2+c/2)l}\right] - \left(\frac{\partial C}{\partial a}\right)_0\left(\frac{\partial a}{\partial w}\right)_0^{+}\frac{1}{2}\left[\frac{1}{p_4}e^{-(p_4/d+\pi c/2d)l}\right],$$

$$a_{21} = \left(\frac{\partial C}{\partial v}\right)_0 \frac{\mu}{2}\left[-\frac{1}{p_2}e^{-(p_2-c/2)l}\right] - \left(\frac{\partial C}{\partial a}\right)_0\left(\frac{\partial a}{\partial w}\right)_0^{-}\frac{1}{2}\left[\frac{1}{p_4}e^{-(p_4/d-\pi c/2d)l}\right],$$

$$a_{22} = -\sigma s - \epsilon k^2 + \mu\left(\frac{\partial C}{\partial v}\right)_0\left[\frac{1}{p_1}(e^{-\lambda_v^{+} l} - 1) + \frac{1}{2p_2}\right] + \left(\frac{\partial C}{\partial a}\right)_0\left(\frac{\partial a}{\partial w}\right)_0^{-}\left[\frac{1}{p_3}(e^{-\lambda_w^{+} l} - 1) + \frac{1}{2p_4}\right]. \quad \text{(A19)}$$

The solution $(\hat{\zeta}_k^{+}(t), \hat{\zeta}_k^{-}(t))$ is formally given as

$$\begin{pmatrix} \hat{\zeta}_k^{+}(t) \\ \hat{\zeta}_k^{-}(t) \end{pmatrix} = \frac{1}{\det(A)}\begin{pmatrix} a_{22} & -a_{12} \\ -a_{21} & a_{11} \end{pmatrix}\begin{pmatrix} -\sigma\zeta_k^{+}(0) \\ -\sigma\zeta_k^{-}(0) \end{pmatrix}, \quad \text{(A20)}$$

where $\det(A) = a_{11}a_{22} - a_{12}a_{21}$. We write $F(s,k) = \det(A)$ in the text. Putting $F(0,k) = 0$, we obtain the bifurcation diagrams, as shown in Figs. 19(a) and 19(b).

We can derive the dependence of solutions on ϵ for sufficiently small ϵ. Under such a situation, we know that $k(\epsilon)$ becomes very large as compared to the other terms, so that

$$\begin{aligned}\det(A) &= a_{11}a_{22} - a_{12}a_{21} \sim a_{11}a_{22} \\ &\sim \left[-\epsilon k^2 + \mu\left(\frac{\partial C}{\partial v}\right)_0\left\{\frac{1}{p_1}(e^{\lambda_v^{-} l} - 1) + \frac{1}{2k}\right\} + \left(\frac{\partial C}{\partial a}\right)_0\left(\frac{\partial a}{\partial w}\right)_0^{+}\left\{\frac{1}{p_3}(e^{\lambda_w^{-} l} - 1) + \frac{1}{2dk}\right\}\right] \\ &\times\left[-\epsilon k^2 + \mu\left(\frac{\partial C}{\partial v}\right)_0\left\{\frac{1}{p_1}(e^{-\lambda_v^{+} l} - 1) + \frac{1}{2k}\right\} + \left(\frac{\partial C}{\partial a}\right)_0\left(\frac{\partial a}{\partial w}\right)_0^{-}\left\{\frac{1}{p_3}(e^{-\lambda_w^{+} l} - 1) + \frac{1}{2dk}\right\}\right] = 0.\end{aligned} \quad \text{(A21)}$$

From Eq. (A21), we note that there are two branches, which are $k(\epsilon) \sim \epsilon^{-1/2}$ in the limit $\epsilon \downarrow 0$.

[1] M. Bode and H.-G. Purwins, Physica D **86**, 53 (1995).
[2] F.-J. Niedernostheide, B. S. Kerner, and H.-G. Purwins, Phys. Rev. B **46**, 7559 (1992).
[3] I. Brauer, M. Bode, E. Ammelt, and H.-G. Purwins, Phys. Rev. Lett. **84**, 4104 (2000).
[4] P. De Kepper, V. Castets, E. Dulos, and J. Boissonade, Physica D **49**, 161 (1991).
[5] K. J. Lee and H. L. Swinney, Phys. Rev. E **51**, 1899 (1995).
[6] D. Haim, G. Li, Q. Ouyang, W. D. McCormick, H. L. Swinney, A. Hagberg, and E. Meron, Phys. Rev. Lett. **77**, 190 (1996).
[7] M. Mimura, H. Sakaguchi, and M. Matsushita, Physica A **282**, 283 (2000).
[8] E. S. Lobanova and F. I. Ataullakhanov, Phys. Rev. Lett. **91**, 138301 (2003).
[9] J. D. Murray, *Mathematical Biology* (Springer-Verlag, Berlin, 1993).
[10] K. J. Lee, W. D. McCormick, Q. Ouyang, and H. L. Swinney, Science **261**, 192 (1993).
[11] J. E. Pearson, Science **261**, 189 (1993).
[12] T. Ohta, M. Mimura, and R. Kobayashi, Physica D **34**, 115 (1989).
[13] J. J. Tyson and J. P. Keener, Physica D **32**, 327 (1988).
[14] E. Meron, Phys. Rep. **218**, 1 (1992).
[15] C. B. Muratov and V. V. Osipov, Phys. Rev. E **54**, 4860 (1996).
[16] C. P. Schenk, P. Schütz, M. Bode, and H.-G. Purwins, Phys. Rev. E **57**, 6480 (1998).
[17] L. M. Pismen, Phys. Rev. Lett. **86**, 548 (2001).
[18] C. Elphick, E. Meron, and E. A. Spiegel, SIAM J. Appl. Math. **50**, 490 (1990).
[19] M. C. Cross and P. C. Hohenberg, Rev. Mod. Phys. **65**, 851 (1993).
[20] T. Ikeda and M. Mimura, J. Math. Biol. **31**, 215 (1993).
[21] M. Suzuki, T. Ohta, M. Mimura, and H. Sakaguchi, Phys. Rev. E **52**, 3645 (1995).
[22] R. Woesler, P. Schütz, M. Bode, M. Or-Guil, and H.-G. Purwins, Physica D **91**, 376 (1996).
[23] M. Or-Guil, M. Bode, C. P. Schenk, and H.-G. Purwins, Phys. Rev. E **57**, 6432 (1998).
[24] S. V. Gurevich, Sh. Amiranashvili, and H.-G. Purwins, Phys. Rev. E **74**, 066201 (2006).
[25] M. Bode, A. W. Liehr, C. P. Schenk, and H.-G. Purwins, Physica D **161**, 45 (2002).
[26] C. P. Schenk, M. Or-Guil, M. Bode, and H.-G. Purwins, Phys. Rev. Lett. **78**, 3781 (1997).
[27] S. V. Gurevich, H. U. Bödeker, A. S. Moskalenko, A. W. Liehr, and H.-G. Purwins, Physica D **199**, 115 (2004).
[28] P. Gray and S. K. Scott, Chem. Eng. Sci. **39**, 1087 (1984).
[29] Y. Nishiura and D. Ueyama, Physica D **150**, 137 (2001).
[30] M. Mimura, M. Nagayama, and T. Ohta, Methods Appl. Anal. **9**, 493 (2002).
[31] T. Ohta, J. Kiyose, and M. Mimura, J. Phys. Soc. Jpn. **66**, 1551 (1997).
[32] T. Ohta, Physica D **151**, 61 (2001).
[33] S. Kawaguchi and M. Mimura, SIAM J. Appl. Math. **59**, 920 (1999).
[34] K. Krischer and A. Mikhailov, Phys. Rev. Lett. **73**, 3165 (1994).
[35] S.-I. Ei, M. Mimura, and M. Nagayama, Discrete Contin. Dyn. Syst. **14**, 31 (2006).